IMA Journal of Applied Mathematics (2019) Page 1 of 18
doi:10.1093/imamat/iarxxx

A second order asymptotic model for Rayleigh waves on a linearly elastic half plane.

PETER T. WOOTTON*
School of Computing and Mathematics, Keele University, Keele, ST5 5BG, UK
School of Mathematics & Statistics, University of Glasgow, Glasgow, G12 8QQ, UK
*Corresponding author: p.t.wootton@keele.ac.uk

JULIUS KAPLUNOV
School of Computing and Mathematics, Keele University, Keele, ST5 5BG, UK
Al-Farabi Kazakh National University, Almaty 050040, Kazakhstan

DANILA PRIKAZCHIKOV
School of Computing and Mathematics, Keele University, Keele, ST5 5BG, UK

[Received on XX XX XXXX; revised on XX XX XXXX; accepted on XX XX XXXX]

We derive a second order correction to an existing leading order model for surface waves in linear elasticity. The same hyperbolic-elliptic equation form is obtained with a correction term added to the surface boundary condition. The validity of the correction term is shown by re-examining problems which the leading order model has been applied to previously, namely a harmonic forcing, a moving point load and a periodic array of compressional resonators.

Keywords: Rayleigh waves, asymptotic, second order.

2000 Math Subject Classification:

1. Introduction

Plane surface waves in linear elasticity, also known as Rayleigh waves Achenbach (1973), are commonly used to model real world problems. Recently this has included a renewed interest in systems involving a forcing along the surface of an infinite bulk, including piezo-electric devices Morgan (1985), non-destructive testing Cho (2003), seismic wave 'lenses' Colombi et al. (2016b), and metasurfaces intended to control and suppress wave propagation Colombi et al. (2016a); Colquitt et al. (2017).

However, unlike bulk waves, these surface waves do not have an explicit wave equation; they are instead 'hidden' through the equations of linear elasticity. This makes both finding the exact solution or undertaking numerical analysis for a system dominated by surface waves difficult. Previous results have shown that the displacement potentials can be expressed as a single function related through harmonic conjugates Friedlander (1948), allowing the Rayleigh wave to be easily found in an arbitrary form Chadwick (1976). This has been extended to surface waves in linear elasticity with general depth dependence Achenbach (1998); Kiselev & Rogerson (2009); Kiselev & Parker (2010). Taking advantage of the relation between displacement potentials, a leading order asymptotic model has been developed for the Rayleigh-type waves produced by forcing along the surface of a linearly elastic half plane, for example see Kaplunov & Prikazchikov (2017).

This model has been applied to multiple problems including: Plane-strain and moving load systems Kaplunov et al. (2010, 2013), mixed boundary problems Erbaş et al. (2012), surface arrays of

rod-like Ege et al. (2018) and beam-like Wootton et al. (2019) resonators, and coated half-space problems Dai et al. (2010). For more general works and further examples see also Kaplunov & Prikazchikov (2017); Nobili & Prikazchikov (2018). In each, the asymptotic model has produced a simple but remarkably accurate approximation of the exact solution. The same asymptotic expansion method has also been applied to produce similar models for interfacial waves in linear elasticity and edge waves on plates Kaplunov & Prikazchikov (2013), piezo-electric waves Kaplunov et al. (2006) and plates with surface loading Erbaş et al. (2018) with similar success.

While this model has proven to give close representations of the exact solution in many cases, as the problems become more involved the deviation between the exact solution and result from the leading order model will increase. This is most notable when there are stresses both parallel and perpendicular to the surface Wootton et al. (2019). As such it is necessary to investigate further development to this model by adding a correction term.

The work shall be arranged as follows: First the leading order model for surface waves in an elastic half plane from Kaplunov & Prikazchikov (2017) will be described, followed by the derivation for a second order model which will add an additional term to the existing model. This new model will then be applied to a variety of simple problems on which the leading order asymptotic model has already been applied. The results from our new model will be compared directly with both the solution from the leading order asymptotic model and the exact solution. The first problem considered will be a simple 2D harmonic forcing. This will be followed by considering a near-resonant moving point load along the surface. Finally we will consider a system originally from Colquitt et al. (2017) consisting of vertical rod-like resonators periodically embedded into the surface of the half plane.

2. Leading Order Asymptotic Model

First we shall summarise the leading order asymptotic model for Rayleigh waves Kaplunov & Prikazchikov (2017). Let there be a linearly elastic half plane with shear and longitudinal displacement potentials ψ and ϕ respectively. From Achenbach (1973) this system has governing equations,

$$\begin{aligned} \phi_{,11} + \phi_{,33} - \frac{1}{c_1^2}\phi_{,tt} = 0, \\ \psi_{,11} + \psi_{,33} - \frac{1}{c_2^2}\psi_{,tt} = 0 \end{aligned} \tag{2.1}$$

where the shear and longitudinal wave speeds are given in terms of the first and second Lamé parameters, λ and μ, and the half plane density, ρ, by

$$c_1 = \frac{\lambda + 2\mu}{\rho}, \qquad c_2 = \frac{\mu}{\rho} \tag{2.2}$$

with surface conditions at $x_3 = 0$,

$$\begin{aligned} 2\phi_{,13} + \psi_{,11} - \psi_{,33} = \frac{Q}{\mu}, \\ (\kappa^{-2} - 2)\phi_{,11} + \kappa^{-2}\phi_{,33} + 2\psi_{,13} = \frac{P}{\mu}. \end{aligned} \tag{2.3}$$

where $\kappa = c_2/c_1$ and Q and P represent some horizontal and vertical surface loading respectively that induce surface wave motion. If the surface loading is small then it follows that the perturbed surface

wave speed, c, will be close to the classical Rayleigh wave speed, c_R. Then a small parameter $0 < \varepsilon \ll 1$ can be defined by,

$$c = c_R(1 \pm \varepsilon). \tag{2.4}$$

and if Q and P are both $O(\varepsilon)$ then ϕ and ψ will have the two-term asymptotic expansions,

$$\phi = \varepsilon^{-1}\phi_0 + \phi_1, \quad \psi = \varepsilon^{-1}\psi_0 + \psi_1, \tag{2.5}$$

where the scale factor ε^{-1} is due to the system resonance for $c = c_R$. Utilising a multiple scales perturbation scheme in the usual way, define independent fast time and slow time variables τ_f and τ_s respectively such that,

$$\tau_f = t, \qquad \tau_s = \varepsilon t, \tag{2.6}$$

leading to the operator identity,

$$\frac{\partial}{\partial t} = \frac{\partial}{\partial \tau_f} + \varepsilon \frac{\partial}{\partial \tau_s}. \tag{2.7}$$

If we use this operator relation to perturb the bulk equations (2.1),

$$\begin{aligned} \phi_{,33} + \alpha_R^2\phi_{,11} - 2\frac{\varepsilon}{c_1^2}\phi_{,\tau_f\tau_s} - \frac{\varepsilon^2}{c_1^2}\phi_{,\tau_s\tau_s} = 0, \\ \psi_{,33} + \beta_R^2\psi_{,11} - 2\frac{\varepsilon}{c_2^2}\psi_{,\tau_f\tau_s} - \frac{\varepsilon^2}{c_2^2}\psi_{,\tau_s\tau_s} = 0. \end{aligned} \tag{2.8}$$

then at $O(\varepsilon^{-1})$,

$$\phi_{0,33} + \alpha_R^2\phi_{0,11} = 0, \qquad \psi_{0,33} + \beta_R^2\psi_{0,11} = 0. \tag{2.9}$$

For a function of the form, $f_{,33} + \gamma^2 f_{,11} = 0$ we can use the harmonic function relations,

$$f_{,3} = -\gamma f^*_{,1}, \qquad f_{,1} = \gamma^{-1} f^*_{,3}, \qquad f^{**} = -f \tag{2.10}$$

where f^* denotes the harmonic conjugate of f. From Chadwick (1976) it is proven that the displacement potentials ϕ and ψ are related by,

$$\psi^* = -\frac{1+\beta_R^2}{2\beta_R}\phi, \qquad \phi^* = \frac{1+\beta_R^2}{2\alpha_R}\psi. \tag{2.11}$$

At $O(1)$ the perturbed bulk equations (2.8) give,

$$\phi_{1,33} + \alpha_R^2\phi_{1,11} = \frac{2}{c_1^2}\phi_{0,\tau_f\tau_s}, \qquad \psi_{1,33} + \beta_R^2\psi_{1,11} = \frac{2}{c_2^2}\psi_{0,\tau_f\tau_s}. \tag{2.12}$$

Assume then that the second order terms of ψ and ϕ are,

$$\phi_1 = \phi_{10} + x_3\phi_{11}, \qquad \psi_1 = \psi_{10} + x_3\psi_{11}, \tag{2.13}$$

and again substituting into the perturbed bulk equations (2.12) yields,

$$\begin{aligned} \phi_{11,31} &= \frac{1}{c_1^2}\phi_{0,1\tau_f\tau_s}, \quad \phi_{11,11} = -\frac{1}{\alpha_R^2 c_1^2}\phi_{0,3\tau_f\tau_s}, \\ \psi_{11,31} &= \frac{1}{c_2^2}\psi_{0,1\tau_f\tau_s}, \quad \psi_{11,11} = -\frac{1}{\beta_R^2 c_2^2}\psi_{0,3\tau_f\tau_s}. \end{aligned} \tag{2.14}$$

Finally, substituting these into the surface conditions (2.3) and taking advantage of the harmonic function relations at $O(1)$ gives, for a small vertical stress (ie. $P = O(1)$, $Q = 0$),

$$2\alpha_R\phi_{10,111} + (1+\beta_R^2)\psi^*_{10,111} = \left(\frac{2}{\alpha_R c_1^2} - \frac{1+\beta_R^2}{\beta_R c_2^2}\right)\phi_{0,1\tau_f\tau_s} \tag{2.15}$$

$$(1+\beta_R^2)\phi_{10,111} + 2\beta_R\psi^*_{10,111} = \left(\frac{2}{c_2^2} - \frac{1+\beta_R^2}{\beta_R^2 c_2^2}\right)\phi_{0,1\tau_f\tau_s} - \frac{P_{,1}}{\mu} \tag{2.16}$$

which gives an expression for the leading order term of ϕ,

$$2\phi_{0,\tau_f\tau_s} = -c_R^2\frac{1+\beta_R^2}{2\mu B}P. \tag{2.17}$$

Similarly, for a horizontal stress (ie. $P = 0$, $Q = O(1)$),

$$2\psi_{0,\tau_f\tau_s} = c_R^2\frac{1+\beta_R^2}{2\mu B}Q. \tag{2.18}$$

3. Second Order Asymptotic Model

We now intend to use the same method to produce a higher order asymptotic model. Continuing the previous expansions (2.5) in the usual way, suppose that ϕ and ψ have the three term asymptotic expansions,

$$\phi = \varepsilon^{-1}\phi_0 + \phi_1 + \varepsilon\phi_2, \quad \psi = \varepsilon^{-1}\psi_0 + \psi_1 + \varepsilon\psi_2. \tag{3.1}$$

We shall first complete the asymptotic treatment for a vertical stress only so let $Q = 0$, $P = \varepsilon P_\varepsilon$. Assume the solution for ϕ_0 (2.17) and relations for the first order non-homogeneous ϕ and ψ terms (2.14) from above. Also assume that ϕ and ψ are related as a single plane harmonic function Chadwick (1976). Taking the perturbed bulk equations (2.8) at $O(\varepsilon)$,

$$\begin{aligned} \phi_{2,33} + \alpha_R^2\phi_{2,11} - \frac{2}{c_1^2}\phi_{1,\tau_f\tau_s} - \frac{1}{c_1^2}\phi_{0,\tau_s\tau_s} = 0, \\ \psi_{2,33} + \beta_R^2\psi_{2,11} - \frac{2}{c_2^2}\psi_{1,\tau_f\tau_s} - \frac{1}{c_2^2}\psi_{0,\tau_s\tau_s} = 0. \end{aligned} \tag{3.2}$$

Supposing that the second order term solutions have the form,

$$\begin{aligned} \phi_2 &= \phi_{20} + x_3\phi_{21} + x_3^2\phi_{22}, \\ \psi_2 &= \psi_{20} + x_3\psi_{21} + x_3^2\psi_{22}, \end{aligned} \tag{3.3}$$

then it follows by substitution that,

$$2\phi_{21,3}+2\phi_{22}+4x_3\phi_{22,3}=\frac{2}{c_1^2}(\phi_{01,\tau_f\tau_s}+x_3\phi_{11,\tau_f\tau_s})+\frac{1}{c_1^2}\phi_{0,\tau_s\tau_s}, \tag{3.4}$$

$$2\psi_{21,3}+2\psi_{22}+4x_3\psi_{22,3}=\frac{2}{c_2^2}(\psi_{01,\tau_f\tau_s}+x_3\psi_{11,\tau_f\tau_s})+\frac{1}{c_2^2}\psi_{0,\tau_s\tau_s}, \tag{3.5}$$

$$\tag{3.6}$$

Matching coefficients in the usual way,

$$2\phi_{22,311}=\frac{1}{c_1^2}\phi_{11,11\tau_f\tau_s},\qquad 2\phi_{21,3}+2\phi_{22}=\frac{2}{c_1^2}\phi_{10,\tau_f\tau_s}+\frac{1}{c_1^2}\phi_{0,\tau_s\tau_s}, \tag{3.7}$$

$$2\psi_{22,311}=\frac{1}{c_2^2}\psi_{11,11\tau_f\tau_s},\qquad 2\psi_{21,3}+2\psi_{22}=\frac{2}{c_2^2}\psi_{10,\tau_f\tau_s}+\frac{1}{c_2^2}\psi_{0,\tau_s\tau_s}. \tag{3.8}$$

Using the relations (2.14) from above yields,

$$2\phi_{22,311}=-\frac{1}{\alpha_R^2c_1^4}\phi_{0,3\tau_f\tau_f\tau_s\tau_s},\qquad 2\psi_{22,311}=-\frac{1}{\beta_R^2c_2^4}\psi_{0,3\tau_f\tau_f\tau_s\tau_s}. \tag{3.9}$$

Assuming that the forcing produces a travelling surface wave, introduce the travelling wave ansatz,

$$\frac{\partial^2}{\partial\tau_f^2}=c_R^2\frac{\partial^2}{\partial x_1^2}, \tag{3.10}$$

which gives,

$$2\phi_{22}=-\frac{c_R^2}{\alpha_R^2c_1^4}\phi_{0,\tau_s\tau_s},\qquad 2\psi_{22}=-\frac{c_R^2}{\beta_R^2c_2^4}\psi_{0,\tau_s\tau_s}, \tag{3.11}$$

and so,

$$2\phi_{21,3}=\frac{2}{c_1^2}\phi_{10,\tau_f\tau_s}+\frac{1}{\alpha_R^2c_1^2}\phi_{0,\tau_s\tau_s}, \tag{3.12}$$

$$2\psi_{21,3}=\frac{2}{c_2^2}\psi_{10,\tau_f\tau_s}+\frac{1}{\beta_R^2c_2^2}\psi_{0,\tau_s\tau_s}. \tag{3.13}$$

Then by using the relations for harmonic functions,

$$2\phi_{21,1}=\frac{2}{\alpha_Rc_1^2}\phi^*_{10,\tau_f\tau_s}+\frac{1}{\alpha_R^3c_1^2}\phi^*_{0,\tau_s\tau_s}, \tag{3.14}$$

$$2\psi_{21,1}=\frac{2}{\beta_Rc_2^2}\psi^*_{10,\tau_f\tau_s}+\frac{1}{\beta_R^3c_2^2}\psi^*_{0,\tau_s\tau_s}. \tag{3.15}$$

Substituting the second order expansions for ϕ and ψ into the boundary conditions and setting $x_3=0$,

$$\begin{aligned}2\phi_{20,13}+(1+\beta_R^2)\psi_{20,11}&=-2\phi_{21,1}+2\psi_{21,3}+2\psi_{22},\\ -(1+\beta_R^2)\phi_{20,11}+2\psi_{20,13}&=-2\frac{1-\beta_R^2}{1-\alpha_R^2}(\phi_{21,3}+\phi_{22})-2\psi_{21,1}.\end{aligned} \tag{3.16}$$

which, on substituting the above relations, yields,

$$2\phi_{20,13}+(1+\beta_R^2)\psi_{20,11}=\frac{2}{c_2^2}\psi_{10,\tau_f\tau_s}+\frac{1}{c_2^2}\psi_{0,\tau_s\tau_s}-\frac{2}{\alpha_R c_1^2}\phi^*_{10,\tau_f\tau_s}-\frac{1}{\alpha_R^3 c_1^2}\phi^*_{0,\tau_s\tau_s}, \tag{3.17}$$

$$2\phi^*_{20,13}+(1+\beta_R^2)\psi^*_{20,11}=\frac{2}{c_2^2}\psi^*_{10,\tau_f\tau_s}+\frac{1}{c_2^2}\psi^*_{0,\tau_s\tau_s}+\frac{2}{\alpha_R c_1^2}\phi_{10,\tau_f\tau_s}+\frac{1}{\alpha_R^3 c_1^2}\phi_{0,\tau_s\tau_s}, \tag{3.18}$$

and,

$$-(1+\beta_R^2)\phi_{20,11}+2\psi_{20,13}=-\frac{1-\beta_R^2}{1-\alpha_R^2}\left(\frac{2}{c_1^2}\phi_{10,\tau_f\tau_s}+\frac{1}{c_1^2}\phi_{0,\tau_s\tau_s}\right)-\frac{2}{\beta_R c_2^2}\psi^*_{10,\tau_f\tau_s}-\frac{1}{\beta_R^3 c_2^2}\psi^*_{0,\tau_s\tau_s}. \tag{3.19}$$

Use the similar leading order relations (2.15) to find a relation for ψ^*_{10} in terms of ϕ_0 and ϕ_{10},

$$\psi^*_{10,11}=-\frac{2\alpha_R}{1+\beta_R^2}\phi_{10,11}+\left(\frac{2}{(1+\beta_R^2)\alpha_R c_1^2}-\frac{1}{\beta_R c_2^2}\right)\phi_{0,\tau_f\tau_s}, \tag{3.20}$$

and using the travelling wave ansatz (3.10),

$$\psi^*_{10,\tau_f\tau_s}=-\frac{2\alpha_R}{1+\beta_R^2}\phi_{10,\tau_f\tau_s}+\left(\frac{2c_R^2}{(1+\beta_R^2)\alpha_R c_1^2}-\frac{c_R^2}{\beta_R c_2^2}\right)\phi_{0,\tau_s\tau_s}, \tag{3.21}$$

Then by taking advantage of relations between harmonic functions,

$$\begin{aligned}2\alpha_R\phi_{20,11}+(1+\beta_R^2)\psi^*_{20,11}=&\left(\frac{2\alpha_R}{1+\beta_R^2}\right)\left(\frac{1+\beta_R^2}{\alpha_R^2 c_1^2}-\frac{2}{c_2^2}\right)\phi_{10,\tau_f\tau_s}\\&+\left(\frac{2\alpha_R}{1+\beta_R^2}\right)\left(\left(\frac{1+\beta_R^2}{2\alpha_R^4}+\frac{1-\beta_R^2}{\alpha_R^2}\right)\frac{1}{c_1^2}-\left(4\frac{1-\beta_R^2}{1+\beta_R^2}+1\right)\frac{1}{c_2^2}\right)\phi_{0,\tau_s\tau_s},\end{aligned} \tag{3.22}$$

$$\begin{aligned}-(1+\beta_R^2)\phi_{20,11}+2\psi_{20,13}=&-\left(\frac{2}{c_2^2}-\frac{1+\beta_R^2}{\beta_R^2 c_2^2}\right)\phi_{10,\tau_f\tau_s}\\&-\left(\frac{1}{c_2^2}+4\frac{1-\alpha_R^2}{(1+\beta_R^2)\alpha_R\beta_R c_2^2}-2\frac{1-\beta_R^2}{\beta_R^2 c_2^2}-\frac{1+\beta_R^2}{2\beta_R^4 c_2^2}\right)\phi_{0,\tau_s\tau_s}.\end{aligned} \tag{3.23}$$

This system of equations can be expressed as,

$$\begin{aligned}2\alpha_R\phi_{20,11}+(1+\beta_R^2)\psi^*_{20,11}&=\left(\frac{2\alpha_R}{1+\beta_R^2}\right)\left(a\phi_{0,\tau_s\tau_s}+b\phi_{10,\tau_f\tau_s}\right),\\-(1+\beta_R^2)\phi_{20,11}-2\beta_R\psi^*_{20,11}&=-\left(c\phi_{0,\tau_s\tau_s}+d\phi_{10,\tau_f\tau_s}\right),\end{aligned} \tag{3.24}$$

where,

$$\begin{aligned}a&=\left(\frac{1+\beta_R^2}{2\alpha_R^4}+\frac{1-\beta_R^2}{\alpha_R^2}\right)\frac{1}{c_1^2}-\left(4\frac{1-\beta_R^2}{1+\beta_R^2}+1\right)\frac{1}{c_2^2}, &\qquad b&=\frac{1+\beta_R^2}{\alpha_R^2 c_1^2}-\frac{2}{c_2^2},\\ c&=\frac{1}{c_2^2}+4\frac{1-\alpha_R^2}{(1+\beta_R^2)\alpha_R\beta_R c_2^2}-2\frac{1-\beta_R^2}{\beta_R^2 c_2^2}-\frac{1+\beta_R^2}{2\beta_R^4 c_2^2}, &\qquad d&=\frac{2}{c_2^2}-\frac{1+\beta_R^2}{\beta_R^2 c_2^2}.\end{aligned} \tag{3.25}$$

Using the Rayleigh identity, this system of equations can then be simplified to,

$$c\phi_{0,\tau_s\tau_s} + d\phi_{10,\tau_f\tau_s} = a\phi_{0,\tau_s\tau_s} + b\phi_{10,\tau_f\tau_s} \tag{3.26}$$

which leads to the relation for the second order component of ϕ,

$$\phi_{10,\tau_f\tau_s} = \frac{a-c}{d-b}\phi_{0,\tau_s\tau_s}, \tag{3.27}$$

$$= \Gamma_R\ \phi_{0,\tau_s\tau_s}, \tag{3.28}$$

where Γ_R can be significantly simplified as,

$$\Gamma_R = 2\frac{1-\beta_R^2}{1+\beta_R^2} - \frac{1}{2} + \frac{1}{2B}\left(2(1-\beta_R^2)^2 + \frac{(\alpha_R^2-\beta_R^2)^2}{\alpha_R^3\beta_R^3}\right), \tag{3.29}$$

which is plotted in Fig [1] for varying values of the Poisson ratio, ν.

To obtain a general relation for ϕ, combine the second order relation (3.28) and the leading order

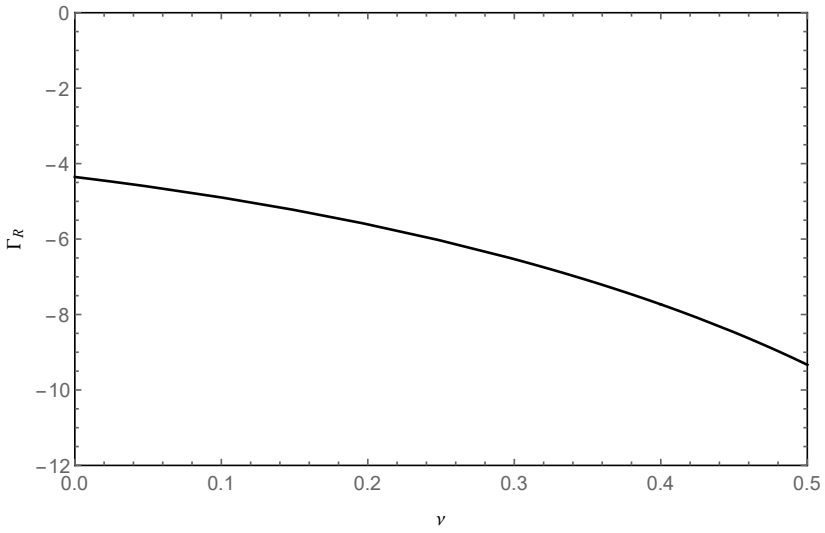

FIG. 1: The values for Γ_R (3.29) for varying Poisson ratio ν.

relation (2.17) to produce,

$$2\varepsilon\phi_{,\tau_f\tau_f\tau_f\tau_s} = -c_R^2\frac{1+\beta_R^2}{2\mu B}\left(P_{,\tau_f\tau_f} + \varepsilon\Gamma_R P_{\tau_f\tau_s}\right). \tag{3.30}$$

Then it follows from the operator relationship (2.7) that,

$$2\varepsilon\frac{\partial^2}{\partial\tau_f\partial\tau_s} = \frac{\partial^2}{\partial t^2} - \frac{\partial^2}{\partial\tau_f^2} - \varepsilon^2\frac{\partial^2}{\partial\tau_s^2}, \tag{3.31}$$

$$= \frac{\partial^2}{\partial t^2} - c_R^2\frac{\partial^2}{\partial x^2} - \varepsilon^2\frac{\partial^2}{\partial\tau_s^2}, \tag{3.32}$$

$$= -c_R^2\Box - \varepsilon^2\frac{\partial^2}{\partial\tau_s^2}. \tag{3.33}$$

which gives,

$$\Box\phi = \frac{1+\beta_R^2}{2\mu B}P - \frac{\varepsilon^2}{c_R^2}(2\Gamma_R+1)\phi_{,\tau_s\tau_s} + 2\frac{\varepsilon^3}{c_R^2}\Gamma_R\phi_{10,\tau_s\tau_s}, \tag{3.34}$$

$$\Box\phi_{,\tau_f\tau_f} = \frac{1+\beta_R^2}{2\mu B}P_{,\tau_f\tau_f} - \frac{\varepsilon^2}{c_R^2}(2\Gamma_R+1)\phi_{,\tau_f\tau_f\tau_s\tau_s} + 2\frac{\varepsilon^3}{c_R^2}\Gamma_R\phi_{10,\tau_f\tau_f\tau_s\tau_s}, \tag{3.35}$$

and the $O(\varepsilon^2)$ term can be expanded using the operator relation,

$$\frac{\varepsilon^2}{c_R^4}\phi_{\tau_f\tau_f\tau_s\tau_s} = \frac{1}{2}\left(\frac{2\varepsilon}{c_R^2}\phi_{0,\tau_f\tau_f\tau_s\tau_s}\right) + O(\varepsilon^3) \tag{3.36}$$

$$= -\frac{1+\beta_R^2}{8\mu B}\left(c_R^2\Box P + \varepsilon^2 P_{,\tau_s\tau_s}\right) + O(\varepsilon^3) \tag{3.37}$$

so on neglecting the remaining $O(\varepsilon^2)$ terms, these can be combined using the travelling wave ansatz (3.10) to give,

$$\Box\phi_{,11} = \frac{1+\beta_R^2}{2\mu B}\left(P_{,11} + \frac{2\Gamma_R+1}{4}\Box P\right), \tag{3.38}$$

or equivalently for a horizontal load,

$$\Box\psi_{,11} = -\frac{1+\beta_R^2}{2\mu B}\left(H_{,11} + \frac{2\Gamma_R+1}{4}\Box H\right). \tag{3.39}$$

From the definition of Γ_R (3.29),

$$\frac{2\Gamma_R+1}{4} = \frac{1-\beta_R^2}{1+\beta_R^2} + \frac{1}{4B}\left(2(1-\beta_R^2)^2 + \frac{(\alpha_R^2-\beta_R^2)^2}{\alpha_R^3\beta_R^3}\right). \tag{3.40}$$

We can verify this using a Taylor expansion around the Rayleigh solution. If the Rayleigh denominator is expressed as a function of $r = c^2/c_2^2$,

$$R(r) = (2-r)^2 - 4\sqrt{1-r}\sqrt{1-\kappa^2 r} \tag{3.41}$$

which has Taylor expansion around the Rayleigh solution $r_0 = c_R^2/c_2^2$,

$$R(r) \approx R(r_0) + R'(r_0)(r-r_0) + \frac{1}{2}R''(r_0)(r-r_0)^2 + ... \tag{3.42}$$

These derivatives are,

$$R'(r) = 2(r-2) + 2\frac{\kappa^2(1-r)+(1-\kappa^2 r)}{\sqrt{1-r}\sqrt{1-\kappa^2 r}}, \tag{3.43}$$

$$R''(r) = 2 + \frac{(1-\kappa^2)^2}{(\sqrt{1-r}\sqrt{1-\kappa^2 r})^3} \tag{3.44}$$

and it is clear that,

$$(r-r_0) = -r_0\left(1-\frac{r}{r_0}\right) = -(1-\beta_R^2)\left(1-\frac{c^2}{c_R^2}\right), \tag{3.45}$$

so for each term of the Taylor series. By definition the leading order term is given by,

$$R(r_0) = 0, \tag{3.46}$$

which as expected represents a solution $R(r) = 0$ at $c = c_R$. The next order term is given by,

$$R'(r_0)(r-r_0) = \left(2(2-r_0) - 2\frac{\kappa^2 r_0(1-r_0)+(1-\kappa^2 r_0)r_0}{\sqrt{1-r_0}\sqrt{1-\kappa^2 r_0}}\right)\left(1-\frac{c^2}{c_R^2}\right), \tag{3.47}$$

$$= -2B\left(1-\frac{c^2}{c_R^2}\right), \tag{3.48}$$

which is the same behaviour as the leading order model. The second order term then takes the form,

$$\frac{1}{2}R''(r_0)(r-r_0)^2 = \left(r_0^2 + \frac{(r_0-\kappa^2 r_0)^2}{2(\sqrt{1-r_0}\sqrt{1-\kappa^2 r_0})^3}\right)\left(1-\frac{c^2}{c_R^2}\right)^2, \tag{3.49}$$

$$= \left((1-\beta_R^2)^2 + \frac{(\alpha_R^2-\beta_R^2)^2}{2\alpha_R^3\beta_R^3}\right)\left(1-\frac{c^2}{c_R^2}\right)^2. \tag{3.50}$$

On combining these expressions we produce the Taylor series,

$$R(r) \approx -2B\left(1-\frac{c^2}{c_R^2}\right)\left(1-\frac{1}{4B}\left(2(1-\beta_R^2)^2 + \frac{(\alpha_R^2-\beta_R^2)^2}{\alpha_R^3\beta_R^3}\right)\left(1-\frac{c^2}{c_R^2}\right)\right), \tag{3.51}$$

which can then be substituted into the previous boundary conditions along the surface. In the case of a vertical stress only,

$$R(r)\phi = -\frac{1+\beta^2}{\mu k^2}P, \tag{3.52}$$

$$\left(1-\frac{c^2}{c_R^2}\right)\phi \approx \frac{1+\beta^2}{2\mu B k^2}\left(1-\frac{1}{4B}\left(2(1-\beta_R^2)^2 + \frac{(\alpha_R^2-\beta_R^2)^2}{\alpha_R^3\beta_R^3}\right)\left(1-\frac{c^2}{c_R^2}\right)\right)^{-1}P, \tag{3.53}$$

$$\approx \frac{1+\beta_R^2}{2\mu B k^2}\left(1+\left(\frac{1-\beta_R^2}{1+\beta_R^2}+\frac{1}{4B}\left(2(1-\beta_R^2)^2 + \frac{(\alpha_R^2-\beta_R^2)^2}{\alpha_R^3\beta_R^3}\right)\right)\left(1-\frac{c^2}{c_R^2}\right)\right)P. \tag{3.54}$$

This clearly has the same form as the dispersion relation obtained above, and by rearranging, the coefficient from the Taylor series matches exactly with the coefficient from the asymptotic expansion.

4. Example Problems

In order to verify that this second order model is valid, we shall next consider three different fundamental types of forcing along the surface and see how the solution obtained from the newly obtained model compares with the result from the previous leading order model and the exact solution. For each, it is expected that the second order model will closely match the exact solution in the vicinity of wave speeds close to the Rayleigh solution and will, in general, be more accurate than the leading order solution.

4.1 *2-Dimensional Harmonic Forcing*

As in Kaplunov & Prikazchikov (2017), introduce a vertical load of constant amplitude,

$$P = P_0 e^{ik(x_1 - ct)}, \tag{4.1}$$

where k is the wave number and as before c is the wave speed. For this forcing the exact solution for ϕ is given by,

$$\phi = \frac{P_0(1+\beta^2)}{\mu k^2 R(c)} e^{ik(x_1 - ct) - k\alpha x_3}, \tag{4.2}$$

with

$$R(c) = (1+\beta^2)^2 - 4\alpha\beta. \tag{4.3}$$

If we define the wave speed by $c = (1+\varepsilon)c_R$ then $c^2 - c_R^2 = (2\varepsilon+\varepsilon^2)c_R^2$ and the leading order asymptotic solution is hence given by,

$$\phi = \frac{P_0(1+\beta_R^2)}{2(2\varepsilon+\varepsilon^2)\mu B k^2} e^{ik(x_1 - ct) - k\alpha_R x_3}. \tag{4.4}$$

We shall repeat the same procedure but use our newly derived second order model (3.38), which yields,

$$\phi = \frac{P_0(1+\beta_R^2)}{2(2\varepsilon+\varepsilon^2)\mu B k^2} \left(1 - \frac{2\Gamma_R + 1}{4}(2\varepsilon+\varepsilon^2)\right) e^{i(kx_1 - ct) - k\alpha_R x_3}. \tag{4.5}$$

It is clear to see that this result is the same as that obtained with the leading order model but with an $O(\varepsilon)$ correction term. To compare the previously obtained results from Kaplunov & Prikazchikov (2017) with that of our new second order model, introduce the scaled potential,

$$\phi_s = \frac{(2\varepsilon+\varepsilon^2)\mu k^2}{2P_0} e^{-ik(x_1 - ct)} \phi(x_1, 0, t). \tag{4.6}$$

where Fig. 2 shows the plots of ϕ_s for both asymptotic models and the exact solution near the Rayleigh speed for a half-plane Poisson ratio of $\nu = 0.25$.

From this figure the improvement of the second order model is clear; while both asymptotic models match exactly with the exact solution at $\varepsilon = 0$, the second order model stays close to the exact solution for a remarkably wide range of wave speeds. It does not however model the mode conversion of the exact solution, where the travelling surface wave solution becomes evanescent and begins to decay along the surface. This is due to treating α and β as fixed constants. In the exact solution as c increases α and β become purely imaginary and the wave propagates into the bulk, a behaviour the asymptotic model cannot replicate.

4.2 *Point Moving Load Steady-State Problem*

Since we have shown that the above model is valid for a static harmonic load, we shall next move to modelling the effects of a moving load. As with before we will make use of a system previously solved

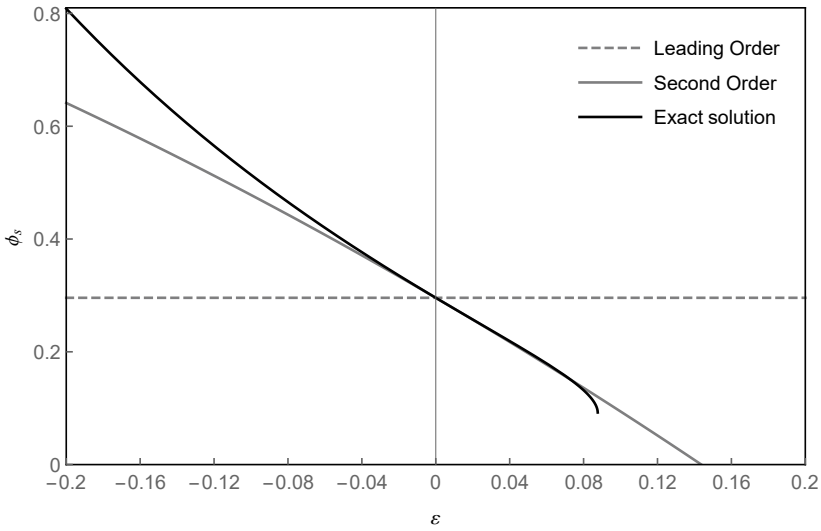

FIG. 2: A comparison of the leading and second order asymptotic models with the exact solution for the scaled potential ϕ_s near the Rayleigh speed for Poisson ratio $\nu = 0.25$. The leading order and second order asymptotic solutions correspond to the dashed grey and solid grey lines respectively and the exact solution is denoted by the solid black line.

using the leading order model Kaplunov et al. (2010); Kaplunov & Prikazchikov (2017), in this instance considering a point vertical load moving at constant speed, c. Using the delta function to represent the point forcing, this load is given by $P = P_0\delta(x_1 - ct)$ along $x_3 = 0$. Introduce a moving coordinate system $s = x_1 - ct$ such that

$$\frac{\partial^2}{\partial x_1^2} = \frac{\partial^2}{\partial s^2}, \qquad \Box = (1-c^2)\frac{\partial^2}{\partial s^2}, \tag{4.7}$$

for which from Kaplunov & Prikazchikov (2017) the leading order asymptotics yields,

$$\phi_{,ss}(s,0) = \frac{1+\beta_R^2}{2\mu B}\frac{c_R^2}{c_R^2 - c^2}P_0\delta(s), \tag{4.8}$$

and so instead at second order,

$$\phi_{,ss}(s,0) = \frac{1+\beta_R^2}{2\mu B}\left(\frac{c_R^2}{c_R^2 - c^2} + \frac{2\Gamma_R + 1}{4}\right)P_0\delta(s). \tag{4.9}$$

This retains the key properties of the leading order model, most notably the resonance at $c = c_R$. This form makes the change from the leading order to the second order model solution relatively straightforward as for constant c, the second order correction acts as a constant multiplicative factor. For instance,

where in Kaplunov & Prikazchikov (2017), the leading order displacement potentials were found to be,

$$\phi_{,s}(s,x_3) = \frac{1+\beta_R^2}{2\pi\mu B}\frac{c_R^2}{c_R^2-c^2}P_0\tan^{-1}\left(\frac{s}{\alpha_R x_3}\right), \tag{4.10}$$

$$\psi_{,s}(s,x_3) = -\frac{\alpha_R}{4\pi\mu B}\frac{c_R^2}{c_R^2-c^2}P_0\ln\left(s^2+\beta_R^2 x_3^2\right), \tag{4.11}$$

from the second order model we instead yield,

$$\phi_{,s}(s,x_3) = \frac{1+\beta_R^2}{2\pi\mu B}\left(\frac{c_R^2}{c_R^2-c^2}+\frac{2\Gamma_R+1}{4}\right)P_0\tan^{-1}\left(\frac{s}{\alpha_R x_3}\right), \tag{4.12}$$

$$\psi_{,s}(s,x_3) = -\frac{\alpha_R}{4\pi\mu B}\left(\frac{c_R^2}{c_R^2-c^2}+\frac{2\Gamma_R+1}{4}\right)P_0\ln\left(s^2+\beta_R^2 x_3^2\right). \tag{4.13}$$

Using the dimensionless variables v, v_R and ξ such that,

$$\xi = \frac{s}{x_3}, \quad v = \frac{c}{c_2}, \quad v_R = \frac{c_R}{c_2}, \tag{4.14}$$

in the same way we can also produce the second order solution for the steady-state displacements,

$$u_1^{st} = \frac{1+\beta_R^2}{2\pi\mu B}\left(\frac{v_R^2}{v_R^2-v^2}-\frac{2\Gamma_R+1}{4}\right)P_0\left(\tan^{-1}\left(\frac{\xi}{\alpha_R}\right)-\frac{1+\beta_R^2}{2}\tan^{-1}\left(\frac{\xi}{\beta_R}\right)\right), \tag{4.15}$$

$$u_2^{st} = -\frac{(1+\beta_R^2)\alpha_R}{4\pi\mu B}\left(\frac{v_R^2}{v_R^2-v^2}-\frac{2\Gamma_R+1}{4}\right)P_0\left(\ln\left(\xi^2+\alpha_R^2\right)-\frac{2}{1+\beta_R^2}\ln\left(\xi^2+\beta_R^2\right)\right). \tag{4.16}$$

As in Kaplunov & Prikazchikov (2017), introduce a scaled stress S_{33} such that,

$$S_{33} = \pi\frac{\sigma_{33}x_3}{P_0}, \tag{4.17}$$

for which the exact solution of the system gives,

$$S_{33} = \frac{\alpha}{R(c)}\left(\frac{(1+\beta^2)^2}{\xi^2+\alpha^2}-\frac{4\beta^2}{\xi^2+\beta^2}\right). \tag{4.18}$$

The leading order asymptotic solution then gives,

$$S_{33} = \frac{2\alpha_R\beta_R}{B}\frac{v_R^2}{v_R^2-v^2}\left(-\frac{\alpha_R}{\xi^2+\alpha_R^2}+\frac{\beta_R}{\xi^2+\beta_R^2}\right) \tag{4.19}$$

and hence it is straightforward to obtain S_{33} from the second order asymptotic solution,

$$S_{33} = \frac{2\alpha_R\beta_R}{B}\left(\frac{v_R^2}{v_R^2-v^2}+\frac{2\Gamma_R+1}{4}\right)\left(-\frac{\alpha_R}{\xi^2+\alpha_R^2}+\frac{\beta_R}{\xi^2+\beta_R^2}\right). \tag{4.20}$$

We shall again compare the leading order solution with the solution obtained from the second order model. This comparison is given in Fig 3 for a Poisson ratio of $\nu = 0.25$, with $v_R \approx 0.9194$, at $\xi = 0.2$. This again shows a significant improvement between the leading order and the exact solution, with the

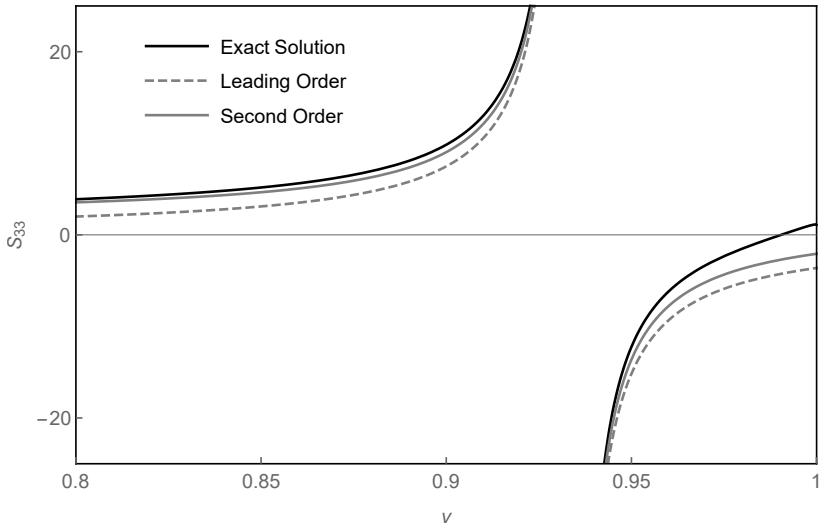

FIG. 3: A comparison of the leading and second order asymptotic models with the exact solution for the scaled stress S_{33} near the Rayleigh speed for a Poisson ratio $\nu = 0.25$ with $\xi = 0.2$. Here the leading order and second order asymptotic solutions correspond to the dashed grey and solid grey lines respectively and the exact solution is denoted by the solid black line.

second order model being a consistent improvement for a wide range of speeds, even those far away from the resonance at the Rayleigh speed. The plot shows that for forcing speeds less than the Rayleigh speed in particular, the second order model approximates the exact solution remarkably well.

Furthermore, the second order model in this instance only introduces a constant multiplying factor to the leading order model. This is a feature of having a forcing of the form $P = P(x_1 - ct)$ and so for any similar moving load problems the second order model will be more accurate than the leading order model but no more difficult to apply.

It is however important to note that this model is only valid near the surface of a near-resonant load, ie. for $c \approx c_R$, and $s \ll x_3$. While when both of these conditions are met the model is shown to be highly accurate, the asymptotic solution cannot predict far-field behaviour or the effect of non-resonant moving loads.

4.3 *Vertical Rod-like Resonators*

We will now attempt to replicate and improve on the results produced by the leading order asymptotic model for a more involved system. From Ege et al. (2018) the asymptotic model was used to accurately interpret the behaviour of a system consisting of a periodic array of identical vertical rod like resonators along the surface of a half plane, originally proposed in Colquitt et al. (2017).

If the spacing between each rod is l then we can introduce the dimensionless variables,

$$K = kl, \quad \Omega = \frac{\omega l}{c_R}, \tag{4.21}$$

where ω and k are respectively the angular frequency and wavenumber of the wave. Hence the exact dispersion relation for this system from Colquitt et al. (2017) can be expressed in dimensionless form in

terms of the Rayleigh denominator (3.41) as,

$$R\left(\frac{c_R\Omega}{c_2K}\right) = 2B\frac{\alpha}{\alpha_R}\left(\frac{\Omega}{K}\right)^3\Upsilon, \tag{4.22}$$

where Υ is a non-dimensional function showing the effect of the resonators, given by,

$$\Upsilon = \frac{d_r}{l}E_r\frac{c_R}{c_r}\alpha_R\frac{\beta_R^2-1}{2\mu B}\tan\left(\frac{h_r\,c_R}{l\,c_r}\Omega\right), \tag{4.23}$$

with d_r, h_r and E_r respectively being the width, height and Young modulus of the resonators and as usual the compressional wave speed of the resonators, c_r, given by $c_r = \sqrt{E_r/\rho_r}$ where ρ_r is the resonator mass density. The leading order asymptotic dispersion relation produced for this system can be expressed as the quadratic equation,

$$K^2 + K\Upsilon\Omega - \Omega^2 = 0. \tag{4.24}$$

Using the second order model introduced above, we instead produce the cubic dispersion relation,

$$K^3 + K^2\left(\frac{2\Gamma_R+5}{4}\right)\Upsilon\Omega - K\Omega^2 - \left(\frac{2\Gamma_R+1}{4}\right)\Upsilon\Omega^3 = 0. \tag{4.25}$$

This dispersion relation is plotted in Fig 4 using the parameters in Table 1. For simplicity, these are the same system parameters as used in the previous treatments of the same problem Colquitt et al. (2017); Ege et al. (2018). Although not immediately clear, it is possible to show that this is the same as the leading order dispersion relation with an $O(\varepsilon)$ correction. Unlike the previous systems however, the second order model requires the solution of a higher order polynomial than the leading order model. While in this case the cubic dispersion relation can still be solved explicitly, this may not be true for other systems where the increase in difficulty to solve the second order model may require numerical or computational solutions.

Table 1: The numerical system parameter values for the rod resonators and half-space used to produce the dispersion relation curves of Figs. 4 and 5.

Symbol	Definition	Value
l	Lattice spacing	2 m
ρ	Half-plane density	13000 kg m^{-3}
μ	Half-plane shear modulus	325 MPa
λ	Half-plane first Lamè parameter	702 MPa
h_r	Resonator length	14 m
d_r	Resonator diameter	0.3m
ρ_r	Resonator density	450 kg m^{-3}
E_r	Resonator Young modulus	1.70 GPa

Fig 4 shows the main behaviours of the exact solution, specifically the resonances at the rod resonant frequency, as well as anti-resonances which intersect the Rayleigh line. However, since both the leading

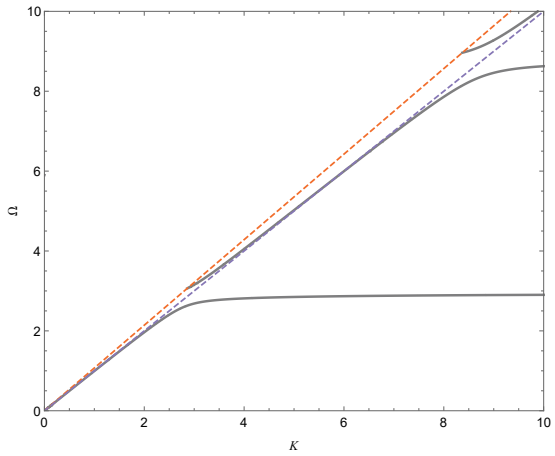

FIG. 4: The second order asymptotic solution (4.25), denoted by the grey curve, for a 2-dimensional system of rod like resonators. The Rayleigh line is plotted in dashed purple and the shear wave line in dashed orange.

order and second order models represent the exact solution near-exactly, it is difficult to determine from this plot whether the second order model is an improvement.

To see if the second order solution is an improvement on the leading order model, we will compare the results of both the leading order and second order model to the exact solution near the system resonances. This comparison is given by Fig 5. These figures show a clear improvement between

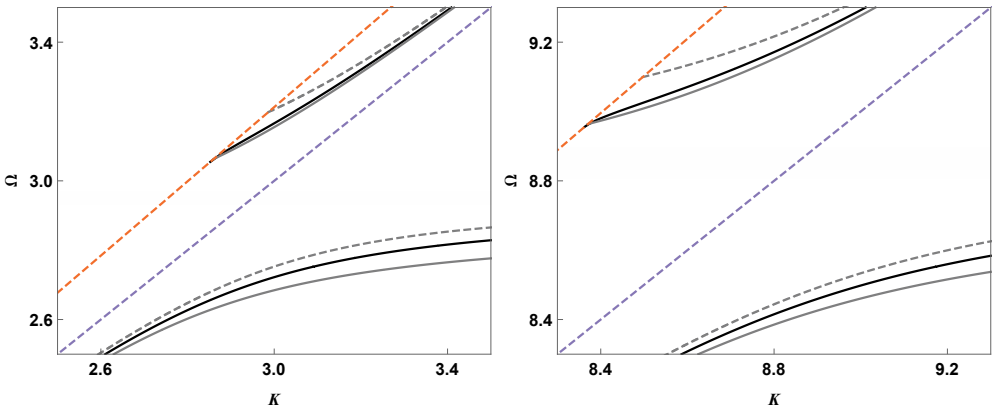

(a) First Asymptote (b) Second Asymptote

FIG. 5: The dispersion relation near the first two resonances for a 2-dimensional system of rod like resonators. The second order asymptotic solution (4.25) is denoted by the solid grey curve, the exact solution (4.22) by the solid black curve, and the first order asymptotic solution (4.24) by the dashed grey curve. The Rayleigh line is plotted in dashed purple and the shear wave line in dashed orange.

the leading order model and the second order model. Between the Rayleigh and shear wave lines in particular the second order model matches with the exact solution remarkably well, with the two solutions almost indistinguishable. Even for larger values of K where the model is predicted to not work as well, the level of matching remains highly accurate with a relative error in Ω of less than $\sim 2\%$ for these material parameters.

5. Concluding Remarks

In this work we have shown that by using the same method used to produce the leading order model for the Rayleigh wave field, it is possible to obtain a higher order correction term to the surface boundary condition while leaving the equations for the bulk unchanged. This correction term leaves the hyperbolic-elliptic nature of the system unchanged with the surface boundary condition still giving a hyperbolic equation. This correction term also converges with the second order Taylor expansion for a surface loading, demonstrating that in a general case the model obtained will converge to the exact solution.

This new higher order model has been applied to three different systems: a vertical harmonic forcing, a steady state point moving load, and an array of vertical resonators attached to the surface. Each of these problems has been treated by the leading order model previously to good effect. Applying the new higher order model to each has shown close matching to the exact solutions and significant improvement over the existing leading order model, at the cost of a less succinct solution form.

The treatment of the harmonic forcing in particular shows how the second order model is an improvement over the leading order model. While the leading order model matches the exact solution only at the Rayleigh speed, the solution from second order model remains a good fit for the exact solution for a much greater range of speeds.

Furthermore, the moving load problem demonstrates how the added accuracy of the model does not necessarily come with an increased difficulty to solve. While the second order model is significantly more accurate than the leading order model, particularly for a wider range of load speeds, the process for solving the problem remains the same.

Finally, the resonator forcing demonstrates how well the second order model can predict the resonances and band gaps caused by a structured surface. This is especially notable as the forcing is not applied, it is caused as a reaction to the existing motion of the half-space, and so the model must accurately represent both the initial motion and the effect of the reaction. These band gaps are particularly sought after for their uses in controlling and suppressing wave propagation and have shown a recent increase in interest in such 'metasurfaces'.

From these results there is clear scope for further development of the model and application of this model in other situations. The leading order model has been extended to full 3D systems and both tangential and perpendicular applied stresses and displacements, and there is no reason why the same cannot be done for the higher order model. Similarly, the higher order model can be used to re-examine previously studied systems to gain further insight and extend those previous systems into more involved problems which the leading order model was not refined enough to accurately approximate. This includes refining the leading order effective parameters obtained for thin film or coating problems, or problems with anisotropy.

Acknowledgment

J. Kaplunov and D Prikazchikov acknowledge support by the Ministry of Education and Science of the Republic of Kazakhstan [IRN AP05132743]. P. Wootton would like to recognise Keele University, UK for supporting his PhD studies.

REFERENCES

Achenbach, J. D. (1973) *Wave propagation in elastic solids*. North-Holland.

Achenbach, J. D. (1998) Explicit solutions for carrier waves supporting surface waves and plate waves. *Wave Motion*, **28**(1), 89–97.

Chadwick, P. (1976) Surface and interfacial waves of arbitrary form in isotropic elastic media. *Journal of Elasticity*, **6**(1), 73–80.

Cho, Y. S. (2003) Non-destructive testing of high strength concrete using spectral analysis of surface waves. *NDT & E International*, **36**(4), 229–235.

Colombi, A., Colquitt, D., Roux, P., Guenneau, S. & Craster, R. V. (2016a) A seismic metamaterial: The resonant metawedge. *Scientific reports*, **6**, 27717.

Colombi, A., Guenneau, S., Roux, P. & Craster, R. V. (2016b) Transformation seismology: Composite soil lenses for steering surface elastic Rayleigh waves. *Scientific reports*, **6**, 25320.

Colquitt, D., Colombi, A., Craster, R., Roux, P. & Guenneau, S. (2017) Seismic metasurfaces: Sub-wavelength resonators and Rayleigh wave interaction. *Journal of the Mechanics and Physics of Solids*, **99**, 379–393.

Dai, H.-H., Kaplunov, J. & Prikazchikov, D. (2010) A long-wave model for the surface elastic wave in a coated half-space. *Proceedings of the Royal Society of London A: Mathematical, Physical and Engineering Sciences*, **466**(2122), 3097–3116.

Ege, N., Erbaş, B., Kaplunov, J. & Wootton, P. (2018) Approximate analysis of surface wave-structure interaction. *Journal of Mechanics of Materials and Structures*, **13**(3), 297–309.

Erbaş, B., Kaplunov, J., Nolde, E. & Palsü, M. (2018) Composite wave models for elastic plates. *Proceedings of the Royal Society A: Mathematical, Physical and Engineering Sciences*, **474**(2214), 20180103.

Erbaş, B., Kaplunov, J. & Prikazchikov, D. A. (2012) The Rayleigh wave field in mixed problems for a half-plane. *The IMA Journal of Applied Mathematics*, **78**(5), 1078–1086.

Friedlander, F. (1948) On the total reflection of plane waves. *The Quarterly Journal of Mechanics and Applied Mathematics*, **1**(1), 376–384.

Kaplunov, J., Nolde, E. & Prikazchikov, D. (2010) A revisit to the moving load problem using an asymptotic model for the Rayleigh wave. *Wave motion*, **47**(7), 440–451.

Kaplunov, J. & Prikazchikov, D. (2013) *Explicit models for surface, interfacial and edge waves*, pages 73–114. Dynamic Localization Phenomena in Elasticity, Acoustics and Electromagnetism. Springer.

Kaplunov, J., Prikazchikov, D., Erbaş, B. & Şahin, O. (2013) On a 3D moving load problem for an elastic half space. *Wave motion*, **50**(8), 1229–1238.

Kaplunov, J. & Prikazchikov, D. A. (2017) *Asymptotic theory for Rayleigh and Rayleigh-type waves*, volume 50 of *Advances in Applied Mechanics*, pages 1–106. Elsevier.

Kaplunov, J., Zakharov, A. & Prikazchikov, D. (2006) Explicit models for elastic and piezoelastic surface waves. *IMA journal of applied mathematics*, **71**(5), 768–782.

Kiselev, A. & Parker, D. (2010) Omni-directional Rayleigh, Stoneley and Schölte waves with general time dependence. *Proceedings of the Royal Society A: Mathematical, Physical and Engineering Sciences*, **466**(2120), 2241–2258.

Kiselev, A. P. & Rogerson, G. A. (2009) Laterally dependent surface waves in an elastic medium with a general depth dependence. *Wave Motion*, **46**(8), 539–547.

Morgan, D. (1985) *Rayleigh Wave Transducers*, pages 60–77. Rayleigh-Wave Theory and Application. Springer.

Nobili, A. & Prikazchikov, D. A. (2018) Explicit formulation for the Rayleigh wave field induced by surface stresses

in an orthorhombic half-plane. *European Journal of Mechanics-A/Solids*, **70**, 86–94.

Wootton, P., Kaplunov, J. & Colquitt, D. (2019) An asymptotic hyperbolic-elliptic model for flexural-seismic metasurfaces. *Proceedings of the Royal Society A: Mathematical, Physical and Engineering Sciences*, **475**(2227).